Behavioral/Systems/Cognitive

Activation of Orexin 1 Receptors in the Periaqueductal Gray of Male Rats Leads to Antinociception via Retrograde Endocannabinoid (2-Arachidonoylglycerol)-Induced Disinhibition

Yu-Cheng Ho (何昱征),[1] Hsin-Jung Lee (李欣蓉),[4] Li-Wei Tung (童力威),[1] Yan-Yu Liao (廖彥昱),[1] Szu-Ying Fu (傅思穎),[1] Shu-Fang Teng (鄧淑方),[2] Hsin-Tzu Liao (廖心慈),[1] Ken Mackie,[6] and Lih-Chu Chiou (邱麗珠)[1,2,3,4,5]

[1]Graduate Institute and [2]Department of Pharmacology, and [3]Graduate Institute of Brain and Mind Sciences, College of Medicine, [4]Graduate Institute of Zoology, [5]Neurobiology and Cognitive Science Center, National Taiwan University, Taipei 100, Taiwan, and [6]Gill Center and the Department of Psychological and Brain Sciences, Indiana University, Bloomington, Indiana 47405

Orexin A and B are hypothalamic peptides known to modulate arousal, feeding, and reward via OX_1 and OX_2 receptors. Orexins are also antinociceptive in the brain, but their mechanism(s) of action remain unclear. Here, we investigated the antinociceptive mechanism of orexin A in the rat ventrolateral periaqueductal gray (vlPAG), a midbrain region crucial for initiating descending pain inhibition. In vlPAG slices, orexin A (30–300 nM) depressed GABAergic evoked IPSCs. This effect was blocked by an OX_1 [1-(2-methylbenzoxazol-6-yl)-3-[1,5]naphthyridin-4-yl urea (SB 334867)], but not OX_2 [*N*-acyl 6,7-dimethoxy-1,2,3,4-tetrahydroisoquinoline hydrochloride (compound 29)], antagonist. Orexin A increased the paired-pulse ratio of paired IPSCs and decreased the frequency, but not amplitude, of miniature IPSCs. Orexin A-induced IPSC depression was mimicked by (*R*)-(+)-[2,3-dihydro-5-methyl-3-(4-morpholinylmethyl)pyrrolo[1,2,3-*de*]-1,4-benzoxazin-6-yl]-1-napthalenylmethanone (WIN 55,212-2), a cannabinoid 1 (CB_1) receptor agonist. 1-(2,4-Dichlorophenyl)-5-(4-iodophenyl)-4-methyl-*N*-(1-piperidyl)pyrazole-3-carboxamide (AM 251), a CB_1 antagonist, reversed depressant effects by both agonists. Orexin A-induced IPSC depression was prevented by 1-[6-[[(17β)-3-methoxyestra-1,3,5(10)-trien-17-yl]amino]hexyl]-1*H*-pyrrole-2,5-dione (U73122) and tetrahydrolipstatin, inhibitors of phospholipase C (PLC) and diacylglycerol lipase (DAGL), respectively, and enhanced by cyclohexyl[1,1′-biphenyl]-3-ylcarbamate (URB602), which inhibits enzymatic degradation of 2-arachidonoylglycerol (2-AG). Moderate DAGLα, but not DAGLβ, immunoreactivity was observed in the vlPAG. Orexin A produced an overall excitatory effect on evoked postsynaptic potentials and hence increased vlPAG neuronal activity. Intra-vlPAG microinjection of orexin A reduced hot-plate nociceptive responses in rats in a manner blocked by SB 334867 and AM 251. Therefore, orexin A may produce antinociception by activating postsynaptic OX_1 receptors, stimulating synthesis of 2-AG, an endocannabinoid, through a Gq-protein-mediated PLC–DAGLα enzymatic cascade culminating in retrograde inhibition of GABA release (disinhibition) in the vlPAG.

Introduction

Orexin A and B (Sakurai et al., 1998), also known as hypocretin 1 and 2 (de Lecea et al., 1998), are endogenous agonists for two Gq-protein-coupled receptors (GqPCRs), OX_1 and OX_2 (Tsujino and Sakurai, 2009). Orexin-expressing neurons are localized in the lateral and perifornical area of the hypothalamus (de Lecea et al., 1998; Sakurai et al., 1998) and send projections widely throughout the CNS (Peyron et al., 1998; van den Pol, 1999). Thus, orexins have been implicated in diverse behaviors and their roles in the regulation of sleep, metabolic homeostasis, and reward have been intensively studied (Tsujino and Sakurai, 2009). Orexins are also antinociceptive at spinal and supraspinal levels in several pain models (Chiou et al., 2010). Endogenous orexins may play a role in stress-induced analgesia (SIA), a neural adaptive response enabling an organism to cope with stress. SIA was attenuated in prepro-orexin knock-out (Watanabe et al., 2005) or orexin neuron-ablated (Xie et al., 2008) mice. However, the mechanisms by which orexins regulate pain remains unclear, especially if they have a role in supraspinal pain control.

The midbrain periaqueductal gray (PAG) is one of the likely supraspinal sites of orexin antinociception. Orexin-containing fibers (Peyron et al., 1998) and OX_1 and OX_2 receptors (Sakurai, 2006) are

Received May 29, 2011; revised Aug. 16, 2011; accepted Aug. 16, 2011.

Author contributions: Y.-C.H., H.-J.L., and L.-C.C. designed research; Y.-C.H., H.-J.L., L.-W.T., Y.-Y.L., S.-Y.F., and S.-F.T. performed research; K.M. contributed unpublished reagents/analytic tools; Y.-C.H., H.-J.L., L.-W.T., Y.-Y.L., S.-Y.F., S.-F.T., K.M., and L.-C.C. analyzed data; Y.-C.H., H.-J.L., S.-F.T., H.-T.L., K.M., and L.-C.C. wrote the paper.

This work was supported by National Science Council (Taipei, Taiwan) Grants NSC 98-2320-B-002-011-MY3, NSC 99-2323-B002-012, and NSC 100-2325-B002-050, National Health Research Institutes (Miaoli, Taiwan) Grant NHRI-EX99-9506NI, National Taiwan University (Taipei, Taiwan) Excellent Research Grant 99R0066-51, and China Medical University (Taichung, Taiwan) Grant 99F008-307 (L.-C.C.), and National Institutes of Health Grants DA011322 and DA021696 (K.M.). We thank Dr. Kenner Rice (Department of Health and Human Services/National Institutes of Health/National Institute on Drug Abuse) for the generous gift of compound 29 and the staff in the Second Core Laboratory, Department of Medical Research, National Taiwan University Hospital, for technical support.

Correspondence should be addressed to Prof. Lih-Chu Chiou, Department of Pharmacology, College of Medicine, National Taiwan University, Number 1, Jen-Ai Road, Section 1, Taipei 100, Taiwan. E-mail: lcchiou@ntu.edu.tw.

DOI:10.1523/JNEUROSCI.2671-11.2011

Copyright © 2011 the authors 0270-6474/11/3114600-11$15.00/0

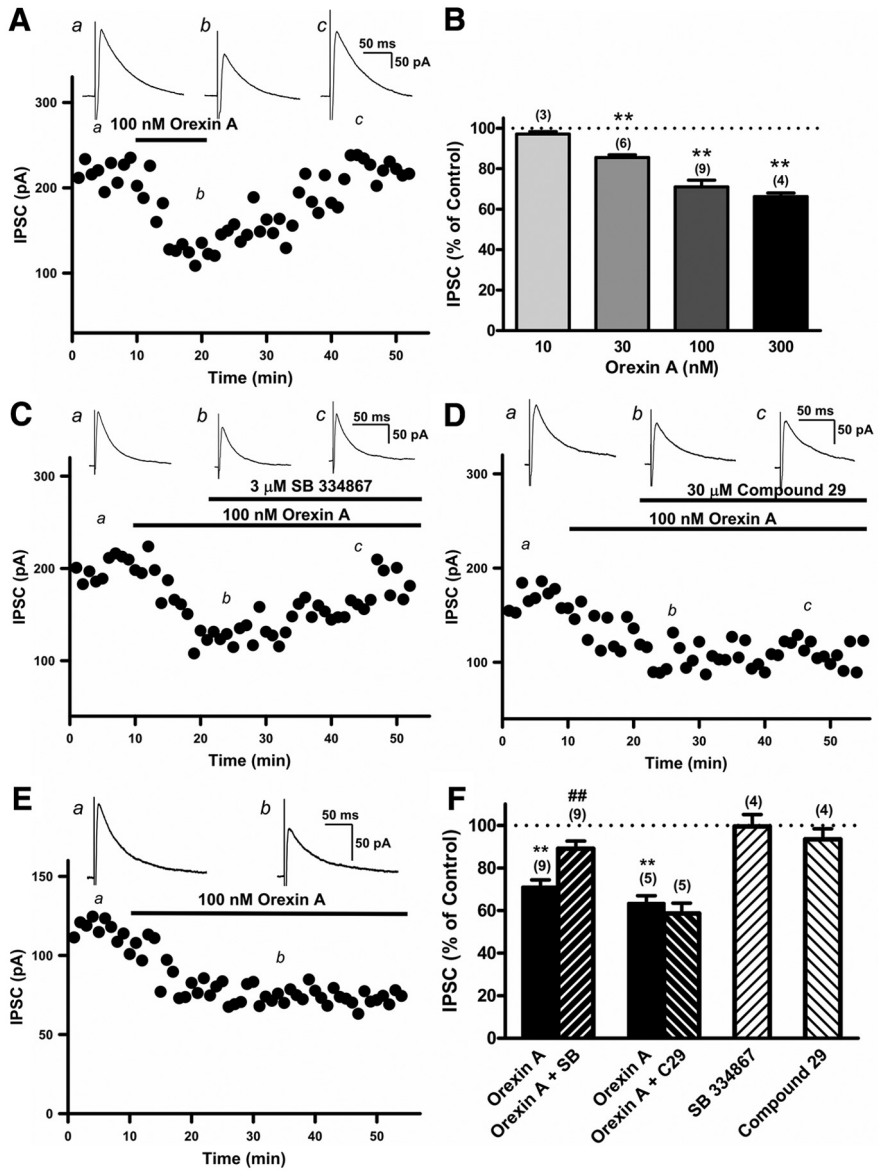

Figure 1. Orexin A depressed IPSCs in a concentration-dependent manner through OX_1, but not OX_2, receptors in vlPAG slices. IPSCs evoked at 0.05 Hz were recorded in the presence of 2 mM kynurenic acid, a glutamate receptor blocker. ***A***, ***C***, ***D***, The time course of the effect of orexin A (100 nM) before (***A***, ***E***) and after further treatment with 3 μM SB 334867 (***C***) or 30 μM compound 29 (***D***) on the amplitude of IPSCs averaged every three IPSCs in a representative vlPAG neuron. Top panels, The averaged IPSC trace taken at the time point *a*, *b*, or *c*. ***B***, Effects of orexin A (10–300 nM) on averaged IPSC amplitude recorded at the steady state, being 10–12 min. $^{**}p < 0.01$ versus control (one-sample *t* test). Note that the effect of orexin A is concentration dependent ($F_{(3,18)} = 16.29$, $p < 0.001$, one-way ANOVA). ***F***, Effects of orexin A (100 nM) before (■) and after further treatment with 3 μM SB 334867 (SB) (▨) or 30 μM compound 29 (C29) (▩). The open bars (▨, ▧) are the groups treated with antagonists alone. $^{**}p < 0.01$ versus control (one-sample *t* test); $^{\#\#}p < 0.01$ versus 100 nM orexin A alone (paired *t* test). The same data presentation and statistical analyses apply to all figures of *in vitro* data. A single bar represents an individual group of neurons with the treatment indicated, and differences between groups were analyzed by Student's *t* test. The grouped bars represent the data from a group of neurons with different treatments conducted sequentially in the same neurons, and the paired *t* test was used for statistical analysis of differences between treatments. One-sample *t* test was used when IPSCs were recorded in the same neuron and normalized to the average IPSC before drug treatment (control) (i.e., the control value was 100%) (Figs. 1*B*, *E*, 4*C*, 5*D*, 6*B*, 10*C*, dotted line). Data are mean ± SEM taken from *n* tested neurons. The *n* number is denoted in the parentheses above each bar.

densely distributed in the PAG (Marcus et al., 2001), and PAG c-*fos* expression was elevated following intracerebroventricular orexin injection (Date et al., 1999). In a preliminary study in mice, we have reported that microinjection of orexin A into the ventrolateral PAG (vlPAG) reduced hot-plate nociceptive responses (Lee and Chiou, 2008). Recently, Azhdari Zarmehri et al. (2011) also reported that, in rats, intra-PAG microinjection of orexin A reduced formalin-induced nociceptive behaviors. Activation of the vlPAG, through inhibition of the tonically active GABAergic circuit (disinhibition), can result in antinociception (Behbehani et al., 1990) by activating a descending pain inhibitory pathway, which originates in the vlPAG, and activates neurons in the rostroventral medulla (RVM), which send inhibitory projections to the dorsal horn of the spinal cord.

Increasing evidence suggests that activation of postsynaptic GqPCRs, such as group I metabotropic glutamate or M_1/M_3 muscarinic receptors (Kano et al., 2009), results in hydrolysis of the plasma membrane lipid, phosphatidylinositol 4,5-bisphosphate, by phospholipase Cβ (PLCβ), yielding diacylglycerol (DAG), which is deacylated by DAG lipase (DAGL) to 2-arachidonoylglycerol (2-AG), an endocannabinoid. 2-AG then diffuses retrogradely to activate the type 1 cannabinoid (CB_1) receptors located on presynaptic nerve terminals, decreasing neurotransmitter release. 2-AG can also be degraded by monoacylglycerol lipase (MGL), which is located in nerve terminals or nearby glia (Kano et al., 2009; Uchigashima et al., 2011). This GqPCR–PLC–DAGL–2-AG retrograde inhibitory signaling module is present in several brain regions, including the PAG (Drew et al., 2008; Lau and Vaughan, 2008; H.-T. Liao et al., 2011).

We, therefore, hypothesized that activation of orexin receptors, which are also GqPCRs, could initiate this GqPCR–PLC–DAGL–2-AG retrograde inhibition onto the tonic GABAergic transmission in the vlPAG, leading to antinociception. In this study, we have validated this hypothesis using a combination of electrophysiological, anatomical, and behavioral approaches.

Materials and Methods

All experiments adhere to the guidelines approved by the Institutional Animal Care and Use Committee of College of Medicine, National Taiwan University.

Electrophysiology

Brain slice preparation. Coronal midbrain slices (400 μm) containing the PAG were dissected from 9- to 18-d-old Wistar rats as described previously (H.-T. Liao et al., 2011; Y.-Y. Liao et al., 2011). After dissection, the slices were equilibrated in artificial CSF (aCSF) at room temperature for at least 1 h before recording. The aCSF contained the following (in mM): 117 NaCl, 4.5 KCl, 2.5 $CaCl_2$, 1.2 $MgCl_2$, 1.2 NaH_2PO_4, 25 $NaHCO_3$, and 11.4 dextrose, and was oxygenated with 95% O_2/5% CO_2, pH 7.4. During recordings, one slice was mounted on a submerged recording chamber and continuously perfused with oxygenated aCSF at a rate of 3–4 ml/min.

Blind patch-clamp recordings. All electrophysiological recordings, except the data in Figure 10, were performed by blind patch-clamp whole-

cell recordings in vlPAG slices using 4–7 MΩ microelectrodes as described previously (Y.-Y. Liao et al., 2011). A K^+-based internal solution containing the following (in mM): 125 K^+ gluconate, 5 KCl, 0.5 $CaCl_2$, 5 BAPTA, 10 HEPES, 5 MgATP, and 0.33 GTP-Tris, pH 7.3, 280 mOsm/L (liquid junction potential, 11.4 mV), was used for recording membrane potentials and evoked postsynaptic potentials (PSPs) in the current-clamp mode. When evoked EPSCs, IPSCs, and miniature IPSCs (mIPSCs) were recorded, a Cs^+-based internal solution was used, which contained the following (in mM): 110 Cs^+ gluconate, 5 TEA (tetraethylammonium), 5 QX314, 0.5 $CaCl_2$, 5 BAPTA, 10 HEPES, 5 MgATP, and 0.33 GTP-Tris (liquid junction potential, 14.6 mV). In one set of experiments, the Ca^{2+}-buffering capacity of the internal solution was increased by elevating the BAPTA concentration to 25 mM. In all cases, liquid junction potentials have been corrected. Electrophysiological signals were acquired and analyzed using an Axon setup (Molecular Devices). Signals were sampled at 5–10 kHz by pClamp 8 via an Axopatch 200B amplifier and Digidata 1200A AD converter and analyzed by Clampfit 8.

Visualized patch-clamp recordings in vlPAG neurons projecting to the RVM. In some experiments (see Fig. 10), visualized whole-cell patch-clamp recordings were performed in those vlPAG neurons that project to the RVM, abbreviated as RVM-vlPAG neurons hereafter. RVM-vlPAG neurons were labeled by a fluorescent retrograde tracer, Red Fluorescent RetroBeads (Lumafluor), injected into the RVM. The rat was anesthetized with 1–2% isoflurane in O_2 and placed in a stereotaxic frame. After the dura was exposed by trephination, the RetroBeads tracer (0.1 μl) was injected over 1 min using a Hamilton syringe (1 μl) into the RVM at the coordinates of DV, −7.5 ∼ −8.5 mm; AP, −1.2 ∼ −1.6 mm (from lambda); ML, −0.0 mm, depending on the age (P8–P15) of the rat. Rats were returned to their holding cages after recovery from anesthesia.

Visualized whole-cell patch-clamp recordings were performed in RVM-vlPAG neurons from brain slices prepared at least 3 d after tracer injection. A stage-fixed upright infrared–differential interference contrast microscope (BX51WI; Olympus) equipped with a 40× water-immersion objective was used. RVM-vlPAG neurons were identified by the presence of red fluorescent beads in the cytoplasm under a rhodamine filter (excitation at 540 mm and emission at 590 mm).

IPSCs, EPSCs, mIPSCs, and PSPs. IPSCs, EPSCs, and PSPs were evoked at 0.05 Hz by a pulse of 10–30 V (150 μs) from a Grass stimulator (Grass Technologies) through a bipolar concentric electrode (FHC) placed 100–200 μm away from the recording electrode to locally stimulate the afferent fiber(s) of the recorded neuron (Chiou and Chou, 2000; H.-T. Liao et al., 2011). IPSCs and mIPSCs were recorded at −40 mV in the presence of 2 mM kynurenic acid, an ionotropic glutamate receptor blocker. When mIPSCs were recorded, tetrodotoxin (TTX), 1 μM, was also added to inhibit action potential-driven spontaneous neurotransmitter release. EPSCs were recorded at −70 mV in the presence of 10 μM bicuculline, a $GABA_A$ receptor blocker. When the paired-pulse ratio (PPR) was examined, paired pulses with 70 ms interstimulus interval were given every 20 s. The PPR was the ratio of averaged amplitude of the second IPSC (IPSC2) to that of the first IPSC (IPSC1).

PSPs were recorded in the current-clamp mode without any receptor blockers in the aCSF or internal solution. In this condition, either depolarizing or hyperpolarizing PSPs could be evoked, depending on the weighting of the stimulated excitatory or inhibitory input of an individual cell, and action potentials were triggered if the depolarizing PSPs reached threshold (Chiou and Huang, 1999; H.-T. Liao et al., 2011).

Every three IPSCs or EPSCs were averaged. The amplitude and trace of averaged IPSCs or EPSCs were used to construct the time course figures (see Figs. 1, 4–6). Stable IPSCs or EPSCs were recorded in each neuron for at least 10 min before an agonist/antagonist was applied. Sometimes an antagonist/agonist was further applied in the same neuron to have a paired comparison in the same neuron. The amplitudes of nine IPSCs or EPSCs were averaged before (the controls) and after drug treatments had reached a steady state, typically 10–12 min. The response after drug treatment in each neuron was expressed as percentage of control. Miniature IPSCs were recorded for 5 min before and at steady state after drug treatments. Mini Analysis 6.0 (Synaptosoft) was used to analyze the amplitude,

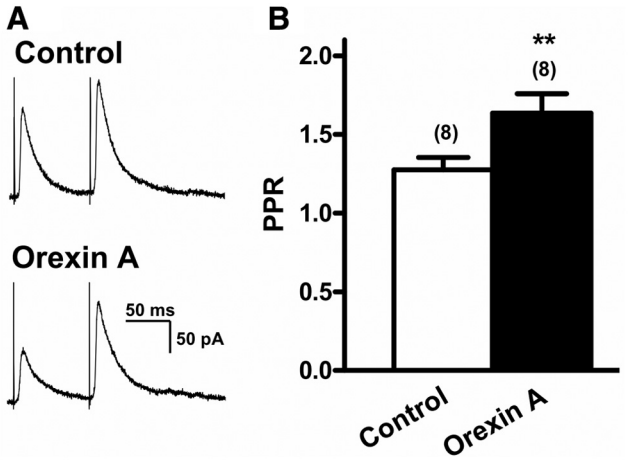

Figure 2. Orexin A increased the PPR of paired IPSCs. ***A***, Paired IPSCs were evoked by 70-ms-separated paired pulses every 20 s. The averaged trace of three paired IPSCs in a neuron before (control) and 10 min after treatment with 100 nM orexin A. ***B***, Averaged PPR, the ratio of the averaged amplitude of second IPSCs to that of first IPSCs, recorded before and after treatment with 100 nM orexin A. $^{**}p < 0.01$ versus control (paired *t* test).

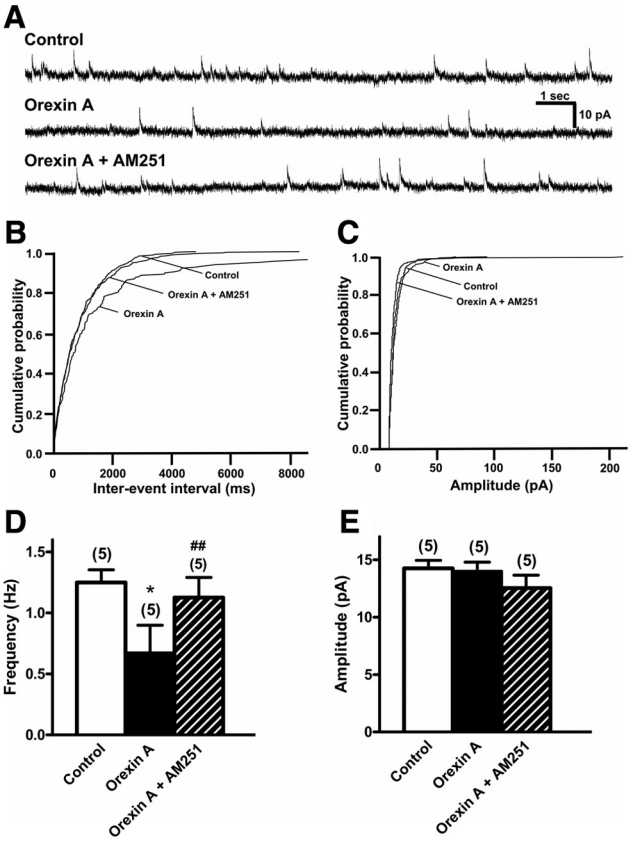

Figure 3. Orexin A decreased the frequency, but not amplitude, of mIPSCs in a manner reversed by a CB_1 antagonist, AM 251. ***A***, mIPSCs recorded in the presence of 2 mM kynurenic acid and 1 μM TTX in a neuron before (top panel) and 10 min after treatment with 100 nM orexin A (middle panel) and further treatment of 3 μM AM 251 (bottom panel). ***B***, ***C***, Cumulative probability of the interval (***B***) or amplitude (***C***) of the mIPSCs recorded for 5 min before and 10 min after treatment with 100 nM orexin A. Data are taken from 370, 177, and 348 mIPSCs in groups of control, orexin A, and orexin A plus AM 251, respectively. Note that orexin A significantly increased the interval ($p < 0.01$, Kolmogorov–Smirnov test) (***B***), but not amplitude (***C***), of mIPSCs in a manner reversed by AM 251. ***D***, ***E***, The average frequency (***D***) and amplitude (***E***) of mIPSCs before and after treatment with orexin A or orexin A plus AM 251. $^{*}p < 0.05$ versus control; $^{\#\#}p < 0.01$ versus 100 nM orexin A alone (paired *t* test).

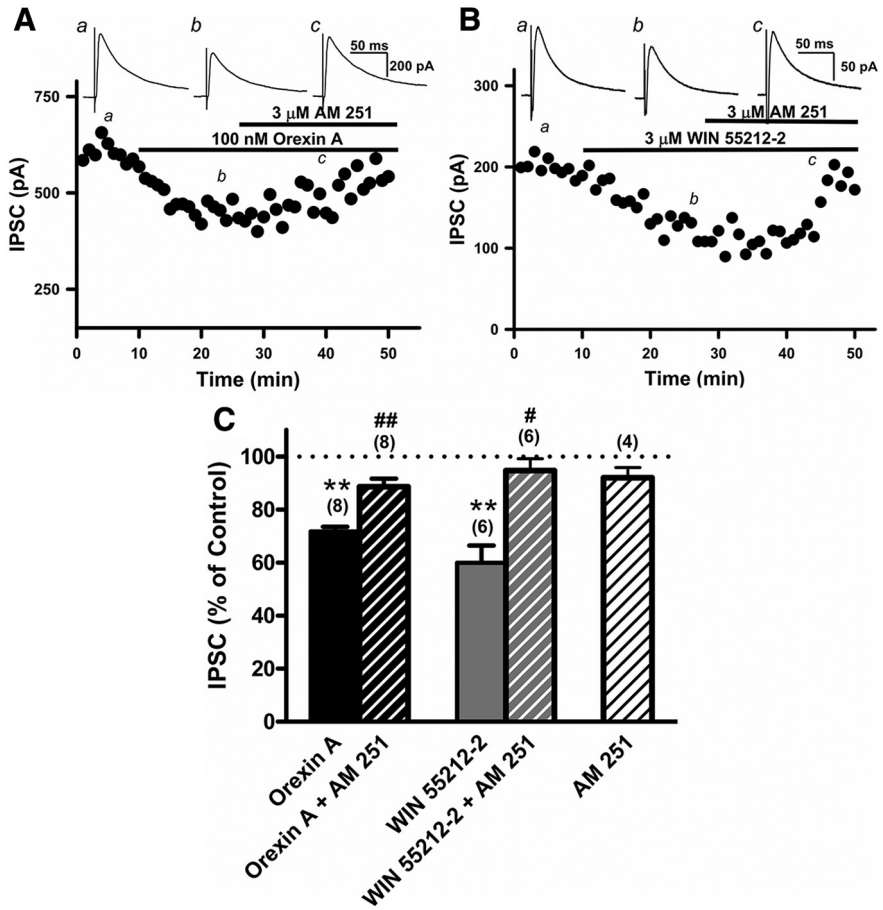

Figure 4. Orexin A-induced IPSC depression was reversed by a CB_1 antagonist, AM 251, and mimicked by a CB_1 agonist, WIN 55,212-2. ***A***, ***B***, The time course of the effect of orexin A (100 nM) (***A***) or WIN 55,212-2 (3 μM) (***B***) on the IPSC amplitude in a representative vlPAG neuron before and after further treatment with AM 251 (3 μM). Top panels, Averaged IPSCs taken before (*a*) and after treatment with orexin A (***A***) or WIN 55,212-2 (***B***) alone (*b*) and in combination with AM 251 (*c*). ***C***, Effect of orexin A (■) or WIN 55,212-2 (■) alone or in combination with AM 251 (▨,▨), or AM 251 alone (▨) on IPSC amplitude. $^{**}p < 0.01$ versus control (one-sample *t* test); $^{\#}p < 0.05$ versus WIN 55,212-2 alone; $^{\#\#}p < 0.01$ versus orexin A alone (paired *t* test).

frequency, and decay time constant of mIPSCs. Kolmogorov–Smirnov test was used to compare the cumulative probability of the frequency and amplitude of mIPSCs between the control and orexin A-treated conditions. One neuron was recorded from one slice, and three to four slices were prepared from each rat.

Immunofluorescent staining

Rats (P9–P18) were anesthetized with sodium pentobarbital (40 mg/kg, i.p.) and then killed by intracardiac perfusion with 4% paraformaldehyde. After perfusion, midbrain blocks containing the PAG were dissected, postfixed for 1 d in the same fixative, and cryoprotected in 30% sucrose overnight. Brain sections of 30 μm were cut with a cryostat (Leica CM3050 S; Leica Microsystems). Sections were then rinsed and washed with PBS three times, followed by 0.3% Triton X-100 containing PBS (PBST) plus 0.5% bovine serum albumin (BSA), and then blocked in PBST containing 1% BSA and 10% normal goat serum for 1 h. Slices were then incubated with the rabbit polyclonal antibodies against DAGLα (diluted 1:500) (Katona et al., 2006) in PBST containing 1% BSA overnight at 4°C. Slices were then washed with PBST three times, followed by incubation with Cy3-conjugated AffiniPure goat anti-rabbit IgG (H+L) (diluted 1:100) (Jackson ImmunoResearch) for 1 h. Fluorescent images were acquired with a Zeiss LSM 510 Meta confocal microscope (Zeiss) and processed with the LSM 510 software (Zeiss).

Behavioral study

All behavioral studies were conducted in male Wistar rats (6–8 weeks of age). Before nociceptive tests, the rat was implanted with a cannula at the vlPAG (AP, −7.8 mm from bregma; LM, −0.5 mm; DV, −6.0 mm). Seven days after cannulation, the rat was subjected to the hot-plate test (50°C) as described previously (H.-T. Liao et al., 2011). The cutoff time was 60 s. Drug solutions of 0.2 μl were delivered into the rat vlPAG through a 30 gauge injection cannula via a 1 μl Hamilton syringe connected to a microinfusion pump (KDS311; KD Scientific). When a receptor antagonist was coinjected with orexin A, twofold concentrated drug solutions were prepared to keep the injection volume at 0.2 μl. Specifically, antagonist solution, 0.1 μl, was injected followed by 0.1 μl of orexin A solution. The injection site was confirmed by injection of trypan blue solution after the hot-plate test. Data from rats with an injection site outside of the vlPAG (offsite injection) were discarded; <7% of tested rats were in this category. To clarify the action site of orexin A, it was intentionally injected in the lateral (AP, −7.8 mm; LM, −0.7 mm; DL, −5.2 mm) and dorsolateral (AP, −7.8 mm; LM, −0.6 mm; DL, −4.5 mm) PAG, respectively, in two groups of rats. The antinociceptive effect of the test drug was evaluated from the area under the curve (AUC) of the withdrawal latencies during the 60 min observation period.

Statistical analyses

Data are expressed as the mean ± SEM, and the *n* number indicates the number of the animals (*in vivo*) or the neurons (*in vitro*) tested. In the *in vitro* study, Student's *t* test was used for statistical comparisons between groups. Paired *t* test was used for different conditions within a group and one-sample *t* test was used for normalized data within a group. One-way ANOVA was used for concentration dependency analysis. In the *in vivo* study, statistical comparisons between groups were analyzed by two-way (Time by Treatment) ANOVA with repeated measures over time and *post hoc* Bonferroni's test for the time courses of their antinociceptive effects, and by Mann–Whitney test for their AUCs. Differences were considered significant if $p < 0.05$.

Chemicals

Orexin A, 1-(2-methylbenzoxazol-6-yl)-3-[1,5]naphthyridin-4-yl urea (SB 334867), (−)-bicuculline methiodide, and 1-[6-[[(17β)-3-methoxyestra-1,3,5(10)-trien-17-yl]amino]hexyl]-1*H*-pyrrole-2,5-dione (U73122) were purchased from Tocris Bioscience. (*R*)-(+)-[2,3-Dihydro-5-methyl-3-(4-morpholinylmethyl)pyrrolo[1,2,3-*de*]-1,4-benzoxazin-6-yl]-1-napthalenylmethanone (WIN 55,212-2), 1-(2,4-dichlorophenyl)-5-(4-iodophenyl)-4-methyl-*N*-(1-piperidyl)pyrazole-3-carboxamide (AM 251), (−)-tetrahydrolipstatin (THL), and kynurenic acid were purchased from Sigma-Aldrich. Cyclohexyl[1,1′-biphenyl]-3-ylcarbamate (URB602) was purchased from Cayman Chemical. *N*-acyl 6,7-dimethoxy-1,2,3,4-tetrahydroisoquinoline hydrochloride (compound 29), a selective OX_2 receptor antagonist (Hirose et al., 2003), was kindly provided by Dr. Kenner Rice (Department of Health and Human Services/National Institutes of Health/National Institute on Drug Abuse, Bethesda, MD). For *in vitro* studies, all drugs were prepared as a 1000-fold concentrated stock solution and diluted to their final concentration with aCSF. For *in vivo* studies, all drugs were prepared as the working concentrations for the intended injection doses. Orexin A and compound 29 were dissolved in deionized water (*in vitro*) or 0.9% normal saline (*in vivo*). Kynurenic acid was dissolved in aCSF directly before use. SB 334867, U73122, WIN 55,212-2, THL, AM 251, and URB602 were dissolved in dimethylsulfoxide (DMSO). The final concentration of DMSO was <0.1%, which had no effect per se.

Results

Orexin A depressed GABAergic IPSCs through OX_1 receptors in vlPAG slices

IPSCs can be evoked in the vlPAG slice treated with kynurenic acid, an ionotropic glutamate receptor blocker, by placing the stimulation electrode 100–200 μm away from the recorded neuron (Chiou and Chou, 2000; H.-T. Liao et al., 2011). These IPSCs are GABAergic since they were blocked by bicuculline, a $GABA_A$ receptor blocker (Chiou and Chou, 2000). Orexin A reversibly depressed these IPSCs (Fig. 1*A*). The effect of orexin A (10–300 nM) was concentration dependent ($p < 0.001$, $F_{(3,18)} = 16.29$, one-way ANOVA) and saturated between 100 and 300 nM (Fig. 1*B*), depressing the IPSCs to 66.2 ± 1.8% of control. Therefore, 100 nM orexin A was used in the following experiments. Orexin A (30–300 nM) depressed IPSCs in almost all (56 of 64; 88%) of the neurons treated with these doses, in which a positive response was taken as a depression >10%.

Orexin A (100 nM)-induced IPSC depression was significantly reversed by SB 334867 (3 μM), an OX_1 antagonist (Fig. 1*C*,*F*). This reversal is not due to a waning of the inhibitory effect of orexin A since, without antagonist, the inhibitory effect of orexin A (100 nM) persisted during a similar recording period, ~40 min (Fig. 1*E*). Conversely, compound 29 (30 μM), an OX_2 antagonist, did not affect orexin A-induced IPSC depression (Fig. 1*D*,*F*). SB 334867 and compound 29 alone had no effect on IPSCs (Fig. 1*F*). These results suggest that orexin A depresses IPSCs in vlPAG slices through OX_1, but not OX_2, receptors.

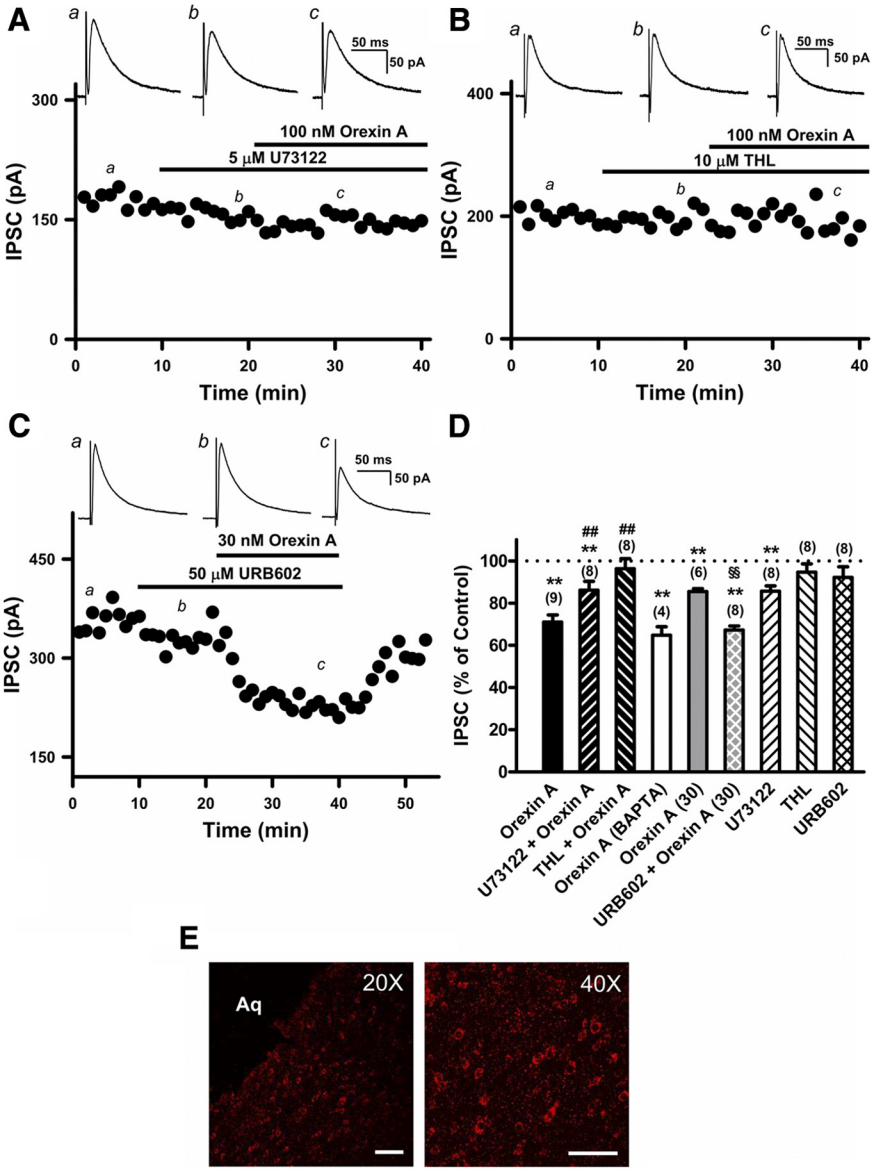

Figure 5. Orexin A-induced IPSC depression was prevented by PLC and DAGL inhibitors and enhanced by an MGL inhibitor. ***A–C***, The time course of the effect of orexin A at 100 nM (***A***, ***B***) or 30 nM (***C***) on the IPSC amplitude in a representative neuron pretreated with U73122 (5 μM; a PLC inhibitor) (***A***), THL (10 μM; a DAGL inhibitor) (***B***), or URB602 (50 μM), an inhibitor of MGL, the major catabolic enzyme of 2-AG, an endocannabinoid (***C***). Top panels, Averaged IPSC taken before (*a*) and after (*b*) treatment with U73122 (***A***), THL (***B***), or URB602 (***C***), and further with orexin A (*c*). ***D***, Effect of orexin A alone (■, 100 nM; ■, 30 nM) or in the presence of PLC (▨), DAGL (▧), or MGL (▩) inhibitor, or effects of inhibitors alone (▨, ▧, ▩) on IPSC amplitude. In a group of neurons, the effect of orexin A (100 nM) was recorded with internal solution containing 25 mM BAPTA to chelate intracellular Ca^{2+} (□). $^{**}p < 0.01$ versus control (one-sample *t* test); $^{\#\#}p < 0.01$ versus 100 nM orexin A alone (Student's *t* test). $^{\S\S}p < 0.01$ versus 30 nM orexin A alone (Student's *t* test). ***E***, Immunofluorescent staining of DAGLα in a PAG section. Immunofluorescent staining demonstrated that DAGLα is moderately distributed in the vlPAG. Aq, Central aqueduct. Scale bars, 100 μm.

Orexin A inhibited GABAergic transmission via a presynaptic mechanism

To elucidate whether presynaptic or postsynaptic mechanism(s) contribute to orexin A-induced IPSC depression, we examined the effect of orexin A on the PPR of paired IPSCs evoked by 70-ms-separated pulses. An altered PPR is consistent with presynaptic modulation (Zucker and Regehr, 2002). Orexin A (100 nM) decreased the amplitude of IPSC1 in paired IPSCs and significantly increased the PPR (Fig. 2*A*,*B*). This suggests orexin A depresses GABAergic IPSCs through a presynaptic mechanism (i.e., by inhibiting evoked GABA release).

We also examined whether orexin A affected postsynaptic receptor responses by examining its effect on mIPSCs. Orexin A (100 nM) did not affect either the amplitude (Fig. 3*A*,*C*,*E*) or the decay time constant (14.3 ± 1.2 vs 15.7 ± 1.2 ms; $n = 5$; $p > 0.05$) of mIPSCs. However, it reduced the frequency of mIPSCs (Fig. 3*A*,*B*,*D*), producing a rightward shift in the cumulative distribution of mIPSC intervals (Fig. 3*B*). These results suggest that orexin A does not affect postsynaptic GABAergic receptors and inhibits synaptic transmission via decreasing presynaptic GABA release.

Orexin A inhibited both evoked and spontaneous GABA release through presynaptic CB_1 receptors

Orexin A is an excitatory modulator of neuronal activity (Chiou et al., 2010); thus, its inhibitory effect on GABAergic transmission is very likely to be indirect. Activation of certain GqPCRs, the GPCR family that the OX_1 receptor belongs to, has been reported to decrease GABA release through the synthesis of endocannabinoids, which retrogradely act on presynaptic CB_1 receptors in

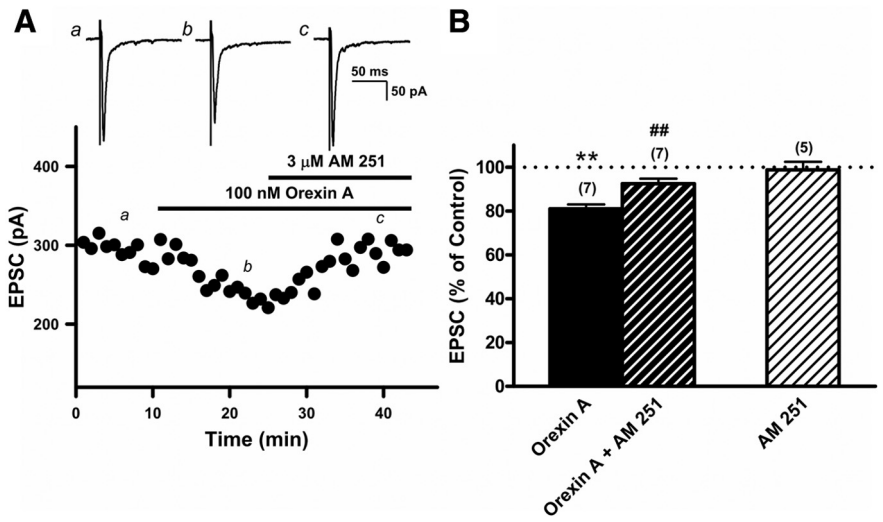

Figure 6. Orexin A also depressed evoked EPSCs in a manner reversed by AM 251 in vlPAG neurons. ***A***, The time course of the effect of orexin A (100 nM) on the EPSC amplitude in a representative vlPAG neuron before and during treatment with AM 251 (3 μM). Top panels, Averaged EPSCs taken before (*a*) and after treatment with orexin A alone (*b*) and in combination with AM 251 (*c*). ***B***, Effect of orexin A (■) alone or in combination with AM 251 (▨), or AM 251 alone (▨) on EPSC amplitude. $^{**}p < 0.01$ versus control (one-sample *t* test); $^{\#\#}p < 0.01$ versus 100 nM orexin A alone (paired *t* test).

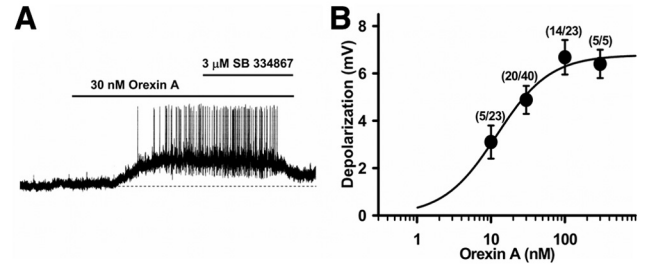

Figure 7. Orexin A induced membrane depolarization in a concentration-dependent fashion in vlPAG neurons. ***A***, The chart recording of the membrane potential in a vlPAG neuron treated with 30 nM orexin A followed by 3 μM SB 334867. Note that the depolarization induced by orexin A was large enough to initiate action potential firings. ***B***, The concentration–response curve of orexin A-induced membrane depolarization. The ordinate is the depolarization induced by orexin A (10–300 nM). The EC_{50} of orexin A estimated from the logistic best-fit curve is 12.3 ± 0.3 nM. The ratio above each data point is the ratio of sensitive neurons to recorded neurons.

several brain regions, including the PAG (Drew et al., 2008; H.-T. Liao et al., 2011). We therefore examined whether orexin A reduced GABA release through CB_1 receptors. Indeed, orexin A (100 nM)-induced IPSC depression was significantly reversed by a CB_1 antagonist, AM 251 (3 μM) (Fig. 4*A*,*C*), and mimicked by a CB_1 agonist, WIN 55,212-2 (Fig. 4*B*,*C*). WIN 55,212-2, at 3 μM, depressed the IPSCs in vlPAG slices to an extent comparable with that produced by 100 nM orexin A (Fig. 4*C*). AM 251 (3 μM) also significantly antagonized the IPSC depressant effect of WIN 55,212-2 (3 μM), a CB_1 agonist (Fig. 4*B*,*C*), but had no effect on IPSCs per se (Fig. 4*C*). In addition, AM 251 also reversed orexin A-induced inhibition of mIPSC frequency (Fig. 3*B*,*D*) but had no effect on mIPSC amplitude (Fig. 3*C*,*E*). These results suggest that orexin A reduces both evoked and spontaneous GABA release indirectly through CB_1 receptors, which have been shown to be located presynaptically in the PAG (Tsou et al., 1998).

Orexin A depressed IPSCs via 2-AG generated through the GqPCR–PLC–DAGL cascade

2-AG is believed to be the endocannabinoid generated via a GqPCR–PLC–DAGL enzymatic cascade after GqPCR activation (Kano et al., 2009). We therefore examined whether orexin A reduced GABA release via OX_1 receptors through a GqPCR– PLC–DAGL cascade. Orexin A inhibition of GABA release was significantly, although incompletely, attenuated by pretreatment with 3 μM U73122 (Fig. 5*A*,*D*), a PLC inhibitor (Bleasdale et al., 1990). The incomplete block by U73122 is likely due to U73122 slightly depressing IPSCs per se (Fig. 5*D*), an effect that was also reported in cultured hippocampal neurons (Hashimotodani et al., 2008). Orexin A-induced IPSC depression was completely prevented by pretreatment with 10 μM THL (Fig. 5*B*,*D*), a DAGL inhibitor (Hadváry et al., 1991), implicating DAGL in orexin A response. Furthermore, URB602 (50 μM), an inhibitor of MGL, the major 2-AG degrading enzyme (Blankman et al., 2007), significantly potentiated the depression of IPSCs induced by a submaximal concentration (30 nM) of orexin A (Fig. 5*C*,*D*). THL and URB602 alone had no significant effect on IPSCs (Fig. 5*D*). Immunofluorescent staining showed that DAGLα, but not DAGLβ (data not shown), was moderately distributed in the vlPAG (Fig. 5*E*). Together, these results suggest that orexin A depresses IPSCs indirectly via 2-AG, an endocannabinoid synthesized via an OX_1–PCL–DAGLα cascade.

Orexin A-induced IPSC depression was unaffected by intracellular Ca^{2+} chelation

Endocannabinoids can also be generated following an elevation of intracellular Ca^{2+} concentration (Kano et al., 2009), a common effect of OX_1 receptor activation (Lund et al., 2000). We therefore examined the effect of orexin A on IPSCs using patch-clamp electrodes filled with an internal solution containing 25 mM BAPTA to rapidly chelate the intracellular Ca^{2+} that would be released upon OX_1 receptor activation. The IPSC depressant effect of orexin A (100 nM) in the neurons recorded with high BAPTA-containing internal solution was not significantly different from that using normal internal solution (64.8 ± 4.0%, $n = 4$, vs 71.0 ± 3.3% of control, $n = 9$; $p = 0.278$) (Fig. 5*D*).

Orexin A also inhibited glutamatergic transmission via endocannabinoids

We next examined whether 2-AG, generated after OX_1 receptor activation, also produced retrograde inhibition of glutamate release in vlPAG slices. In the presence of bicuculline (10 μM), a $GABA_A$ receptor blocker, EPSCs can be evoked by local stimulation in vlPAG slices (Chiou and Chou, 2000). Orexin A (100 nM) also depressed EPSCs in a manner reversed by AM 251 (3 μM) (Fig. 6*A*). AM 251 had no effect on EPSC amplitude per se (Fig. 6*B*). However, EPSCs, compared with IPSCs, were significantly less depressed by orexin A. The mean amplitudes of EPSCs and IPSCs after treatment with 100 nM orexin A were 80.9 ± 2.0% ($n = 7$) and 71.0 ± 3.3% ($n = 9$) of control, respectively ($p < 0.05$, unpaired *t* test) (compare Figs. 6*B*, 5*D*).

Orexin A caused an OX_1 receptor-mediated membrane depolarization in approximately one-half of vlPAG neurons

Orexin A (10–300 nM) caused membrane depolarization in a concentration- dependent fashion. Cells showing a consistent depolarization of >1 mV were considered to be depolarized. Among 91 neurons treated with 10–300 nM orexin A, 41 neurons (45%) were depolarized by this criterion (Fig. 7*A*,*B*). There were no significant differences in the resting membrane potential (−65.2 ± 0.9 vs −66.9 ± 1.3 mV) or input resistance (194 ± 32 vs 184 ± 37 MΩ) between orexin A-sensitive and -insensitive neurons.

The depolarization induced by orexin A could be as much as 6–7 mV and could ultimately initiate action potentials (Fig. 7*A*). The EC_{50} of orexin A-induced depolarization, estimated from the concentration–response curve, was 12.3 ± 0.3 nM (Fig. 7*B*). SB 334867 (3 μM) did not affect membrane potential per se (data not shown) but significantly antagonized orexin A-induced membrane depolarization and action potentials (Fig. 7*A*).

Orexin A exerted an overall excitatory effect on vlPAG neuronal activity

We further investigated the net effect of orexin A on the neuronal activity evoked by presynaptic stimulation in vlPAG slices. Presynaptic stimulation can evoke either depolarizing or hyperpolarizing PSPs in recorded neurons, depending on the weighting of glutamatergic or GABAergic inputs (Chiou and Huang, 1999; H.-T. Liao et al., 2011). Among a total of 26 recorded neurons, depolarizing PSPs were evoked in 23 neurons and hyperpolarizing PSPs were evoked in 3 neurons. Orexin (100 nM) caused membrane depolarization in 15 of 26 neurons. In addition to membrane depolarization (Fig. 8*A*,*B*,*D*,*E*), orexin A exerted an excitatory effect on evoked PSPs, either by enhancing depolarizing PSPs (Fig. 8*A*,*C–E*) or depressing hyperpolarizing PSPs (Fig. 8*B*). The excitatory effect of orexin A was sufficient for the presynaptic stimulation to elicit action potentials (Fig. 8, middle column) whether the membrane potential was depolarized (Fig. 8*A*,*B*,*D*,*E*) or not (Fig. 8*C*). After correcting the depolarized membrane potentials to control levels (right column), the PSPs were still large enough to trigger action potentials after treatment with orexin A, whether or not they were depolarizing (Fig. 8*A*) or hyperpolarizing (Fig. 8*B*) PSPs before treatment. Interestingly, AM 251 blocked the PSP enhancement and subsequent action potential generation, but not membrane depolarization, induced by orexin A (Fig. 8*D*). However, SB 334867 blocked both effects induced by orexin A (Fig. 8*E*). These results suggest the neuronal excitatory effect of orexin A is mainly attributable to its inhibition of GABAergic transmission, although postsynaptic depolarization, which is endocannabinoid independent, may also contribute to the increased network excitability.

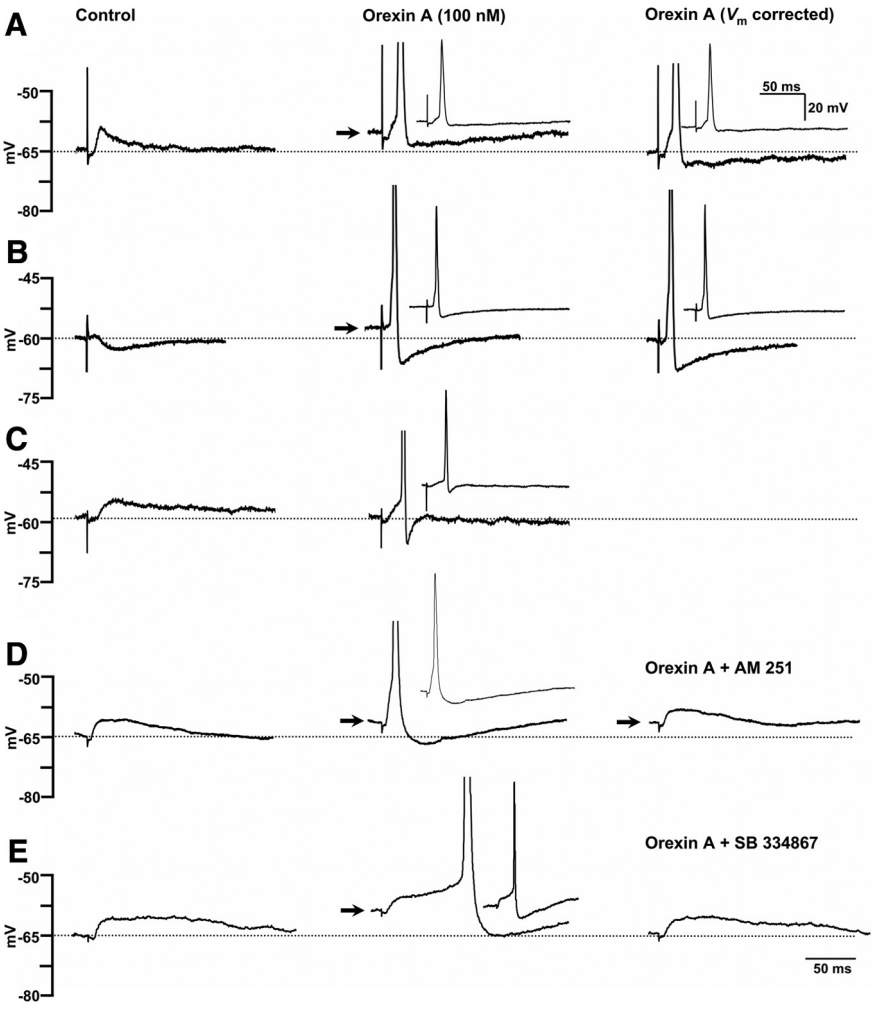

Figure 8. Orexin A exerted an overall excitatory effect on the vlPAG neuronal activity. PSPs evoked at 0.05 Hz by presynaptic stimulation were recorded in the current-clamp mode without any receptor blocker. Either depolarizing PSPs (***A***, ***C***, ***D***, ***E***) or hyperpolarizing PSP (***B***) could be evoked in the control. Orexin A (100 nM) induced membrane depolarization in some neurons (***A***, ***B***, ***D***, ***E***). It also produced an excitatory effect on PSPs, whether or not depolarizing (***A***, ***C***, ***D***, ***E***) or hyperpolarizing (***B***) PSPs were initially evoked, and ultimately triggered action potentials. After correcting the depolarized membrane potentials (arrows) to the control levels (dotted lines), the PSPs were still large enough to trigger action potentials in the presence of orexin A (right column). Action potentials are shown in the insets with lower calibration scales. ***D***, ***E***, The representative neuron, in which orexin A had induced depolarization and elicited action potentials, was subsequently treated with AM 251 (3 μM) (***D***) or SB 334867 (3 μM) (***E***). Note that AM 251 blocked the excitatory effect on PSPs and the subsequent neuronal activity, but not depolarization (arrows), induced by orexin A (***D***). However, SB 334867 (3 μM) blocked both effects (***E***).

Intra-vlPAG microinjection of orexin A induced antinociception via CB_1 receptors

To verify that the actions of orexin A observed in PAG slices can contribute to its antinociceptive effect, we performed an *in vivo* study using the hot-plate pain model in rats. Orexin A was injected, at 0.1, 0.3, 1, and 3 nmol, into the vlPAG. Rats receiving off-site injections (outside the vlPAG) and those injections intentionally conducted in the dorsolateral and lateral PAG had no response to orexin A (Fig. 9*B*, inset, open circles). These data were not included in our behavioral analysis. Orexin A significantly increased the withdrawal latency in the rat hot-plate test, as indicated by a main effect of Treatment ($F_{(3,84)} = 64.83$; $p < 0.001$, two-way ANOVA with repeated measures over time) (Fig. 9*A*). The antinociceptive effect of orexin A was time dependent, as

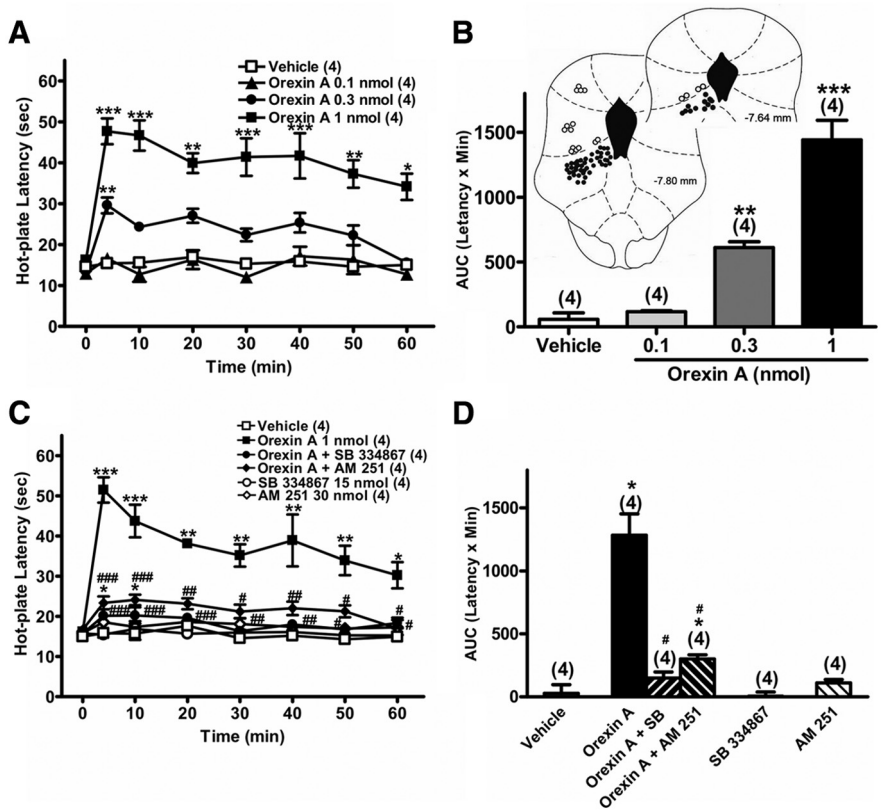

Figure 9. Intra-vlPAG microinjection of orexin A in rats induced antinociception via OX_1 receptor-activated endocannabinoid retrograde signaling via CB_1 receptors in the paw withdrawal hot-plate test. All drugs were given by intra-vlPAG microinjection. The paw withdrawal cutoff time was 60 s. Data are the averaged antinociceptive effect in each treatment group at the same time point. ***A***, The time course of the hot-plate withdraw latency in rats treated with vehicle (□) or 0.1 nmol (▲), 0.3 nmol (●), or 1 nmol (■) of orexin A. Two-way ANOVA with repeated measures over time analysis indicated significant differences with a main effect of Treatment ($F_{(3,84)} = 64.83$; $p < 0.001$) and of Time ($F_{(7,84)} = 13.31$; $p < 0.001$), and in the interaction of Treatment by Time ($F_{(21,84)} = 5.020$; $p < 0.001$). $^{*}p < 0.05$, $^{**}p < 0.01$, $^{***}p < 0.001$ versus the vehicle group (*post hoc* Bonferroni's comparisons of the data points denoted). ***B***, The antinociceptive effect, expressed as the AUC of the hot-plate withdrawal latencies during the 60 min recording period, in the group treated with vehicle or orexin A (0.1–1 nmol). Inset, Microinjection sites taken from all rats with successful injections (●) and offsite injections (○), including those intentionally injected into the lateral and dorsolateral PAG, were depicted in two PAG sections at bregma −7.64 and −7.80 mm, respectively. Injection sites were confirmed by trypan blue injected through the microinjection cannula after the hot-plate test. The numbers in the parentheses are the number of rats tested for each condition. $^{**}p < 0.01$, $^{***}p < 0.001$ versus the vehicle group ($F_{(3,12)} = 44.31$, one-way ANOVA with *post hoc* Dunnett's test). ***C***, The time course of the hot-plate withdraw latency in rats treated with vehicle (□), orexin A (1 nmol) (■), orexin A plus SB 334867 (15 nmol) (●), orexin A plus AM 251 (30 nmol) (◆), SB 334867 alone (○), or AM 251 alone (◇). Note that SB 334867 and AM 251 significantly decreased the antinociceptive effect induced by orexin A (Treatment, $F_{(5,126)} = 39.65$, $p < 0.001$; Time, $F_{(7,126)} = 15.75$, $p < 0.001$; Treatment by Time, $F_{(35,126)} = 6.564$, $p < 0.001$, two-way ANOVA with repeated measures over time). $^{*}p < 0.05$, $^{**}p < 0.01$, $^{***}p < 0.001$ versus the vehicle group; $^{\#}p < 0.05$, $^{\#\#}p < 0.01$, $^{\#\#\#}p < 0.001$ versus orexin A-only group (*post hoc* Bonferroni's comparisons of the data points denoted). ***D***, The antinociceptive effect, expressed as AUC, of orexin A (1 nmol) in the presence or absence of SB 334867 (15 nmol) or AM 251 (30 nmol). $^{*}p < 0.05$ versus the vehicle group; $^{\#}p < 0.05$ versus orexin A-only group (Mann–Whitney test).

indicated by a main effect of Time ($F_{(7,84)} = 13.31$; $p < 0.001$). The interaction of Treatment by Time was also significantly different ($F_{(21,84)} = 5.020$; $p < 0.001$). *Post hoc* analysis (Bonferroni's test) showed that the effect of orexin at 0.3 and 1 nmol was dose and time dependent. The effect at 1 nmol reached its peak within 5 min of injection, and then gradually decreased, but lasting for >60 min (Fig. 9*A*,*C*). The duration was reduced with decreasing doses of orexin A (0.3 nmol) (Fig. 9*A*). Orexin A, at 3 nmol, caused motor impairment. Therefore, 1 nmol of orexin A was used for subsequent experiments. The antinociceptive effect of orexin A was antagonized by intra-vlPAG microinjection of both OX_1 and CB_1 antagonists, as indicated by a main effect of Treatment ($F_{(5,126)} = 39.65$; $p < 0.001$, two-way ANOVA with repeated measures over time). The antagonist effects were persistent ($F_{(35,126)} = 6.564$; $p < 0.001$). *Post hoc* analysis (Bonferroni's test) showed that SB 334867 (15 nmol) completely antagonized the effect of orexin A (Fig. 9*C*,*D*), while AM 251, at 30 nmol, significantly reduced, but did not completely abolish, the antinociceptive effect of orexin A (Fig. 9*C*,*D*), especially immediately after (10 min) orexin A injection (Fig. 9*C*). At this dose, AM 251 completely abolished the antinociceptive effect of WIN 55,212-2, a CB_1 agonist (H.-J. Lee and L.-C. Chiou, unpublished observation). Neither antagonist per se changed withdrawal latency (Fig. 9*C*,*D*). These data supported the notion that 2-AG retrograde signaling induced by OX_1 receptor activation contributes to the antinociceptive effect of orexin A in the vlPAG by primarily acting at CB_1 receptors.

Orexin A also induced a CB_1 receptor-dependent depression of IPSCs in RVM-vlPAG neurons

Activation of the vlPAG could also result in antinociception through ascending circuits (Morgan et al., 1989) in addition, or as an alternative, to activating the descending inhibitory pathway. We therefore examined whether orexin A also depressed IPSCs in vlPAG neurons projecting to the RVM, an important downstream node in the descending pain inhibitory pathway (Heinricher et al., 2009). RVM-vlPAG neurons were identified by the presence of fluorescent RetroBeads in the cytoplasm following their injection into the RVM (Fig. 10*A*). The fluorescence observed using a rhodamine filter (Fig. 10*Ab*) was sufficiently strong to be visible with conventional bright-field optics (Fig. 10*Ac*). In RVM-PAG neurons, orexin A (100 nM) also depressed IPSCs (Fig. 10*B*). The magnitude of depression was similar to that obtained in randomly selected vlPAG neurons, 70.8 ± 4.7% ($n = 5$) versus 71.0 ± 3.3% ($n = 9$) of control ($p = 0.97$, unpaired t test). This depressant effect was also significantly reversed by AM 251 (3 μM) (Fig. 10*B*). These results suggest that orexin A inhibits IPSCs via endocannabinoids acting at CB_1 receptors in vlPAG neurons projecting to the RVM.

Discussion

In this study, our findings suggest that activation of postsynaptic OX_1 receptors in the vlPAG can initiate a Gq protein-coupled PLCβ–DAGLα enzymatic pathway to generate 2-AG, an endocannabinoid that may travel across the synapse to inhibit GABA release through presynaptic CB_1 receptors, a disinhibition phenomenon (Fig. 11). This disinhibition mechanism in the vlPAG, likely via activating the descending pain inhibitory pathway, can contribute to the antinociceptive effect of orexin A in the vlPAG.

To the best of our knowledge, this is the first study revealing the interplay between the orexin and endocannabinoid systems in pain processing.

Orexin A, via OX_1 receptors, decreases GABA release through endocannabinoids

The finding that orexin A-induced IPSC depression in vlPAG neurons was antagonized by SB 334867, but not compound 29, suggests it is mediated through OX_1, but not OX_2, receptors. The IPSCs evoked by local stimulation in the vlPAG are GABAergic since they were blocked by bicuculline (Chiou and Chou, 2000). Since orexin A is an excitatory modulator of neuronal activity (van den Pol et al., 1998), it is unlikely that orexin A directly inhibited GABAergic transmission. The effectiveness of AM 251 in reversing orexin A-depressed IPSCs suggests an involvement of CB_1 receptors, which have been demonstrated on GABAergic terminals in the PAG (Tsou et al., 1998). The findings that orexin A increased the PPR of paired IPSCs and decreased mIPSC frequency further substantiate that the IPSC depressant effect of orexin A is of presynaptic origin. We also showed that WIN 55,212-2 (a synthetic CB_1 agonist) mimicked the effect of orexin A, depressing IPSCs in PAG slices as previously observed (Vaughan et al., 2000). These results suggest that orexin A indirectly decreases GABA release by the production of endocannabinoids that engage CB_1 receptors on GABAergic terminals.

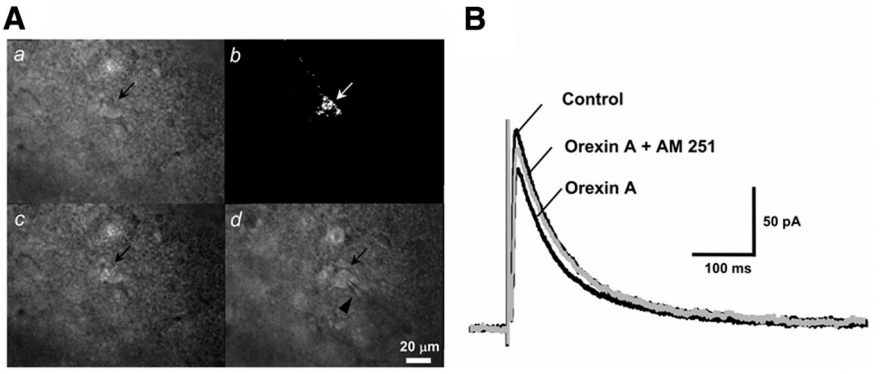

Figure 10. Orexin A induced a CB_1 receptor-dependent depression of IPSCs in vlPAG neurons projecting to the rostral ventromedulla (RVM-vlPAG neurons). RVM-vlPAG neurons were retrogradely labeled by injecting red fluorescent RetroBeads into the RVM of rats 3 d before preparing brain slices for *in vitro* recordings. ***A***, Photomicrographs of a RVM-vlPAG neuron taken before recording without (*a*) or with (*b*, *c*) fluorescence illumination, and during recording with the recording electrode (*d*). Note that the fluorescence observed using a rhodamine filter (*b*) was sufficiently strong to be visible with conventional bright-field optics (*c*). ***B***, Representative IPSCs recorded from an RVM-vlPAG neuron taken before (Control) and after treatment with 100 nM orexin A, alone (Orexin A), or in combination with 3 μM AM 251 (Orexin A + AM 251).

2-AG synthesized through the GqPCR–PLCβ–DAGLα cascade after postsynaptic OX_1 receptor activation is the endocannabinoid producing retrograde inhibition of GABA release

Endocannabinoids are generally synthesized on demand at postsynaptic sites and may be generated when certain GqPCRs are activated (Kano et al., 2009). Here, we demonstrated that orexin A-induced IPSC depression was prevented by inhibitors of PLC and DAGL, and identified DAGLα to be present in the PAG. DAGLα, an important enzyme for synthesizing 2-AG (Tanimura et al., 2010), was found to be broadly located postsynaptically in somata or dendrites, but not in presynaptic terminals (Ludányi et al., 2011; Uchigashima et al., 2011). These data suggest that orexin A depresses IPSCs through 2-AG, which is synthesized from DAG by postsynaptic DAGLα after PLC activation upon engagement of OX_1 receptors (Fig. 11). The finding that orexin A-induced IPSC depression was enhanced by inhibition of MGL, a major 2-AG degrading enzyme located in presynaptic terminals (Hashimotodani et al., 2007; Uchigashima et al., 2011), further suggests that 2-AG synthesized at postsynaptic site diffuses retrogradely to activate CB_1 receptors and inhibit GABA release and then be degraded by presynaptic MGL (Fig. 11).

It has been shown that 2-AG retrograde inhibition can be triggered in the vlPAG by activating postsynaptic GqPCRs, such as M_1/M_3 muscarinic (Lau and Vaughan, 2008) and group I mGlu (Drew et al., 2008; H.-T. Liao et al., 2011) receptors. We now show that endocannabinoid retrograde signaling in the vlPAG can also be triggered by OX_1 receptor activation and mediates the antinociceptive effect of orexin A in this region. Retrograde endocannabinoid inhibition initiated by orexin B has been reported in the dorsal raphe, but the orexin receptor subtype involved was not identified and the endocannabinoid inhibited glutamate release (Haj-Dahmane and Shen, 2005) rather than GABA release as observed in the vlPAG.

OX_1 receptor-mediated 2-AG inhibition of GABA release is not spatially restricted

The 2-AG generated after postsynaptic OX_1 receptor activation through the GqPCR–PLCβ–DAGLα cascade may either diffuse retrogradely to the presynaptic terminal of the same synapse (Fig. 11, right) or spread to nearby GABAergic terminals of other synapses (Fig. 11, left) to inhibit GABA release via presynaptic CB_1 receptors. This inference is based on the finding that orexin A depressed IPSCs in almost all (88%) of the recorded neurons but caused membrane depolarization in only one-half (45%) of them. The ineffectiveness of intracellular BAPTA in preventing orexin A-induced IPSC depression in the recorded neuron further supports that 2-AG was synthesized and diffused from nearby neurons, instead of from only the recorded neuron, upon OX_1 receptor activation. Additionally, immunohistochemical studies demonstrated that OX_1 receptors are expressed in a limited subset of PAG neurons (Hervieu et al., 2001), and not as intensively as CB_1 receptors (Tsou et al., 1998).

Heterosynaptic endocannabinoid spread has been found to contribute to depolarization-induced suppression of inhibition in the hippocampus (Wilson and Nicoll, 2001), amphetamine-induced long-term depression in the amygdala (Huang et al., 2003), and the Purkinje cell activation-induced inhibition of interneuron firing in the cerebellum (Kreitzer et al., 2002). Here, we provided further evidence supporting the phenomenon of heterosynaptic endocannabinoid spread in the vlPAG after OX_1 receptor activation. It will be interesting to determine whether this efficient inhibition induced by heterosynaptic endocannabinoid spread after OX_1 receptor activation also exists in other brain regions.

Orexin A excites the vlPAG mainly via 2-AG retrograde disinhibition

The finding that orexin A also depressed EPSCs in a manner blocked by a CB_1 antagonist suggests that 2-AG generated after OX_1 receptor activation also produces retrograde inhibition of

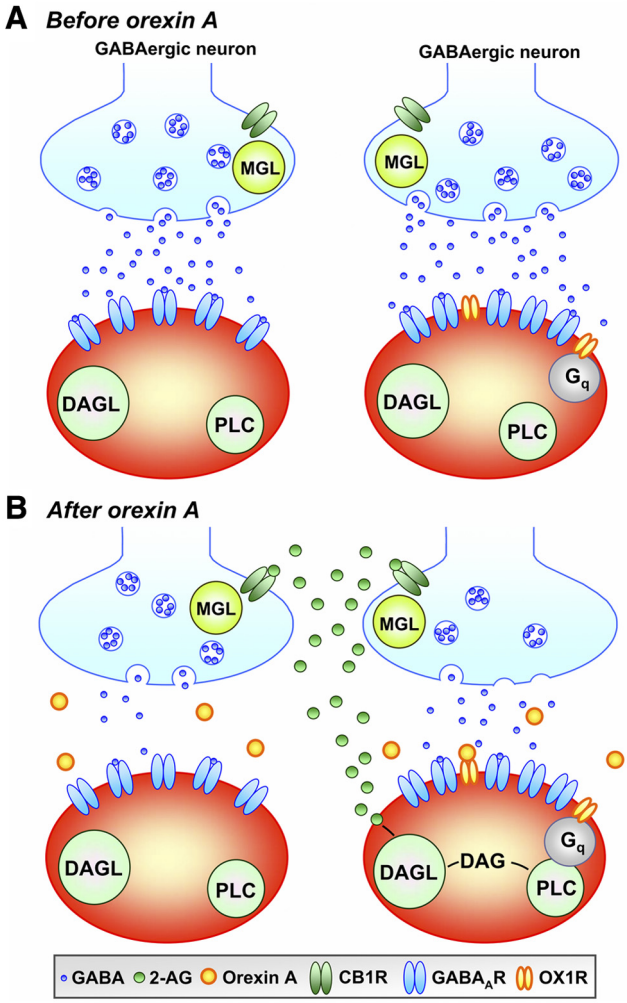

Figure 11. A proposed model for how orexin A-induced inhibition of GABAergic transmission in the vlPAG ultimately leads to antinociception by activating the descending pain inhibitory pathway. The schema shows two GABAergic innervated neurons, with (right) and without (left) postsynaptic OX_1 receptors in the vlPAG before (***A***) and after (***B***) treatment with orexin A. Orexin A activates postsynaptic OX_1 receptors in the vlPAG neuron (right) and then, coupled by Gq protein, stimulates PLC to yield DAG which can be deacylated by DAGLα to 2-AG, an endocannabinoid. 2-AG subsequently activates the presynaptic CB_1 receptors located on the GABAergic terminal of the same neuron as a retrograde messenger (right) or the CB_1 receptors on the adjacent GABAergic terminal as a heterosynaptic spillover messenger (left) to inhibit GABA release. Inhibition of the GABAergic transmission (disinhibition) in the vlPAG will activate the descending pain inhibitory pathway and reduce nociceptive responses. 2-AG can be degraded by the MGL located in GABAergic terminals. Thus, the MGL inhibitor enhances orexin A-induced IPSC depression.

excitatory transmission. However, orexin A depressed IPSCs to a greater extent than EPSCs, suggesting a more profound inhibition by orexin A on GABAergic than glutamatergic transmission. This preferential inhibitory effect of endocannabinoids on GABA, rather than glutamate, transmission was also observed in the hippocampus (Ohno-Shosaku et al., 2002) and basal amygdaloid nucleus (Yoshida et al., 2011). This preferential GABAergic inhibition may contribute to the overall excitatory effect of orexin A on PSPs and on subsequent neuronal activity (Fig. 8). Furthermore, AM 251 blocked orexin A-induced neuronal activity but not depolarization (Fig. 8*D*). It is, therefore, suggested that the neuronal excitatory effect of orexin A is mainly attributable to its indirect inhibition of GABAergic transmission via CB_1 receptors, although postsynaptic depolarization, which is endocannabinoid independent, may also contribute to increased network excitability.

Antinociceptive mechanism of orexin A in the vlPAG

Antinociception can be induced by directly exciting the vlPAG or by inhibiting intrinsic GABAergic tone (disinhibition) (Behbehani et al., 1990), to activate the descending pain inhibitory pathway. The finding that intra-vlPAG microinjection of orexin A increased the hot-plate latency in the rat confirms the vlPAG to be an important site of action for orexin-induced supraspinal antinociception (Lee and Chiou, 2008; Azhdari Zarmehri et al., 2011). This antinociceptive effect of orexin A was markedly reduced by cotreatment with AM 251, suggesting that the disinhibition produced by retrograde 2-AG after OX_1 receptor activation plays a major role in orexin A-induced antinociception in the vlPAG. This inference is further supported by the generalized elevated neuronal activity in vlPAG slices treated with orexin A. However, the postsynaptic depolarizing effect of orexin A, which could ultimately lead to neuronal firing, may also partly contribute to its antinociceptive effect in the vlPAG. This contention is supported by a slight residual antinociceptive effect of orexin A in rats cotreated with AM 251 (Fig. 9).

Excitation of the PAG might also induce antinociception via ascending analgesic pathways (Morgan et al., 1989). The possibility that orexin A might excite the PAG to induce analgesia through this ascending mechanism(s) cannot be conclusively ruled out. However, the finding that orexin A depressed IPSCs in vlPAG neurons projecting to the RVM (Fig. 10) provides direct evidence supporting the hypothesis that orexin A can excite the PAG to activate the descending pain inhibitory pathway.

Functional role of this analgesic mechanism of orexin A

The present study reveals a novel analgesic mechanism in the vlPAG through activation of the orexin system followed by 2-AG generation. This orexin-dependent analgesic mechanism may contribute to SIA since endogenous orexins have been suggested to play a role in the generation of SIA (Watanabe et al., 2005; Xie et al., 2008) and SIA is believed to involve endocannabinoids within the PAG (Hohmann et al., 2005). The orexin neurons in the lateral hypothalamus send projections to the PAG. Therefore, during stress, hypothalamic orexin neurons may be activated; released orexins then activate the OX_1 receptor in the vlPAG to produce analgesia through 2-AG via the GqPCR–PLCβ–DAGLα cascade.

References

Azhdari Zarmehri H, Semnanian S, Fathollahi Y, Erami E, Khakpay R, Azizi H, Rohampour K (2011) Intra-periaqueductal gray matter microinjection of orexin-A decreases formalin-induced nociceptive behaviors in adult male rats. J Pain 12:280–287.

Behbehani MM, Jiang MR, Chandler SD, Ennis M (1990) The effect of GABA and its antagonists on midbrain periaqueductal gray neurons in the rat. Pain 40:195–204.

Blankman JL, Simon GM, Cravatt BF (2007) A comprehensive profile of brain enzymes that hydrolyze the endocannabinoid 2-arachidonoylglycerol. Chem Biol 14:1347–1356.

Bleasdale JE, Thakur NR, Gremban RS, Bundy GL, Fitzpatrick FA, Smith RJ, Bunting S (1990) Selective inhibition of receptor-coupled phospholipase C-dependent processes in human platelets and polymorphonuclear neutrophils. J Pharmacol Exp Ther 255:756–768.

Chiou LC, Chou HH (2000) Characterization of synaptic transmission in the ventrolateral periaqueductal gray of rat brain slices. Neuroscience 100:829–834.

Chiou LC, Huang LY (1999) Mechanism underlying increased neuronal activity in the rat ventrolateral periaqueductal grey by a mu-opioid. J Physiol 518:551–559.

Chiou LC, Lee HJ, Ho YC, Chen SP, Liao YY, Ma CH, Fan PC, Fuh JL, Wang SJ (2010) Orexins/hypocretins: pain regulation and cellular actions. Curr Pharm Des 16:3089–3100.

Date Y, Ueta Y, Yamashita H, Yamaguchi H, Matsukura S, Kangawa K, Sakurai T, Yanagisawa M, Nakazato M (1999) Orexins, orexigenic hypothalamic peptides, interact with autonomic, neuroendocrine and neuroregulatory systems. Proc Natl Acad Sci U S A 96:748–753.

de Lecea L, Kilduff TS, Peyron C, Gao X, Foye PE, Danielson PE, Fukuhara C, Battenberg EL, Gautvik VT, Bartlett FS 2nd, Frankel WN, van den Pol AN, Bloom FE, Gautvik KM, Sutcliffe JG (1998) The hypocretins: hypothalamus-specific peptides with neuroexcitatory activity. Proc Natl Acad Sci U S A 95:322–327.

Drew GM, Mitchell VA, Vaughan CW (2008) Glutamate spillover modulates GABAergic synaptic transmission in the rat midbrain periaqueductal grey via metabotropic glutamate receptors and endocannabinoid signaling. J Neurosci 28:808–815.

Hadváry P, Sidler W, Meister W, Vetter W, Wolfer H (1991) The lipase inhibitor tetrahydrolipstatin binds covalently to the putative active site serine of pancreatic lipase. J Biol Chem 266:2021–2027.

Haj-Dahmane S, Shen RY (2005) The wake-promoting peptide orexin-B inhibits glutamatergic transmission to dorsal raphe nucleus serotonin neurons through retrograde endocannabinoid signaling. J Neurosci 25:896–905.

Hashimotodani Y, Ohno-Shosaku T, Kano M (2007) Presynaptic monoacylglycerol lipase activity determines basal endocannabinoid tone and terminates retrograde endocannabinoid signaling in the hippocampus. J Neurosci 27:1211–1219.

Hashimotodani Y, Ohno-Shosaku T, Maejima T, Fukami K, Kano M (2008) Pharmacological evidence for the involvement of diacylglycerol lipase in depolarization-induced endocanabinoid release. Neuropharmacology 54:58–67.

Heinricher MM, Tavares I, Leith JL, Lumb BM (2009) Descending control of nociception: specificity, recruitment and plasticity. Brain Res Rev 60:214–225.

Hervieu GJ, Cluderay JE, Harrison DC, Roberts JC, Leslie RA (2001) Gene expression and protein distribution of the orexin-1 receptor in the rat brain and spinal cord. Neuroscience 103:777–797.

Hirose M, Egashira S, Goto Y, Hashihayata T, Ohtake N, Iwaasa H, Hata M, Fukami T, Kanatani A, Yamada K (2003) *N*-Acyl 6,7-dimethoxy-1,2,3,4-tetrahydroisoquinoline: the first orexin-2 receptor selective nonpeptidic antagonist. Bioorg Med Chem Lett 13:4497–4499.

Hohmann AG, Suplita RL, Bolton NM, Neely MH, Fegley D, Mangieri R, Krey JF, Walker JM, Holmes PV, Crystal JD, Duranti A, Tontini A, Mor M, Tarzia G, Piomelli D (2005) An endocannabinoid mechanism for stress-induced analgesia. Nature 435:1108–1112.

Huang YC, Wang SJ, Chiou LC, Gean PW (2003) Mediation of amphetamine-induced long-term depression of synaptic transmission by CB_1 cannabinoid receptors in the rat amygdala. J Neurosci 23:10311–10320.

Kano M, Ohno-Shosaku T, Hashimotodani Y, Uchigashima M, Watanabe M (2009) Endocannabinoid-mediated control of synaptic transmission. Physiol Rev 89:309–380.

Katona I, Urbán GM, Wallace M, Ledent C, Jung KM, Piomelli D, Mackie K, Freund TF (2006) Molecular composition of the endocannabinoid system at glutamatergic synapses. J Neurosci 26:5628–5637.

Kreitzer AC, Carter AG, Regehr WG (2002) Inhibition of interneuron firing extends the spread of endocannabinoid signaling in the cerebellum. Neuron 34:787–796.

Lau BK, Vaughan CW (2008) Muscarinic modulation of synaptic transmission via endocannabinoid signalling in the rat midbrain periaqueductal gray. Mol Pharmacol 74:1392–1398.

Lee HJ, Chiou LC (2008) Antinociceptive action of orexins given by microinjection at the ventrolateral periaqueductal gray in the mouse hot plate test. Soc Neurosci Abstr 34:826.12.

Liao HT, Lee HJ, Ho YC, Chiou LC (2011) Capsaicin in the periaqueductal gray induces analgesia via metabotropic glutamate receptor-mediated endocannabinoid retrograde disinhibition. Br J Pharmacol 163:330–345.

Liao YY, Teng SF, Lin LC, Kolczewski S, Prinssen EP, Lee LJ, Ho IK, Chiou LC (2011) Functional heterogeneity of nociceptin/orphanin FQ receptors revealed by (+)-5a compound and Ro 64-6198 in rat periaqueductal grey slices. Int J Neuropsychopharmacol 14:977–989.

Ludányi A, Hu SS, Yamazaki M, Tanimura A, Piomelli D, Watanabe M, Kano M, Sakimura K, Maglóczky Z, Mackie K, Freund TF, Katona I (2011) Complementary synaptic distribution of enzymes responsible for synthesis and inactivation of the endocannabinoid 2-arachidonoylglycerol in the human hippocampus. Neuroscience 174:50–63.

Lund PE, Shariatmadari R, Uustare A, Detheux M, Parmentier M, Kukkonen JP, Akerman KE (2000) The orexin OX1 receptor activates a novel Ca^{2+} influx pathway necessary for coupling to phospholipase C. J Biol Chem 275:30806–30812.

Marcus JN, Aschkenasi CJ, Lee CE, Chemelli RM, Saper CB, Yanagisawa M, Elmquist JK (2001) Differential expression of orexin receptors 1 and 2 in the rat brain. J Comp Neurol 435:6–25.

Morgan MM, Sohn JH, Liebeskind JC (1989) Stimulation of the periaqueductal gray matter inhibits nociception at the supraspinal as well as spinal level. Brain Res 502:61–66.

Ohno-Shosaku T, Tsubokawa H, Mizushima I, Yoneda N, Zimmer A, Kano M (2002) Presynaptic cannabinoid sensitivity is a major determinant of depolarization-induced retrograde suppression at hippocampal synapses. J Neurosci 22:3864–3872.

Peyron C, Tighe DK, van den Pol AN, de Lecea L, Heller HC, Sutcliffe JG, Kilduff TS (1998) Neurons containing hypocretin (orexin) project to multiple neuronal systems. J Neurosci 18:9996–10015.

Sakurai T (2006) Roles of orexins and orexin receptors in central regulation of feeding behavior and energy homeostasis. CNS Neurol Disord Drug Targets 5:313–325.

Sakurai T, Amemiya A, Ishii M, Matsuzaki I, Chemelli RM, Tanaka H, Williams SC, Richardson JA, Kozlowski GP, Wilson S, Arch JR, Buckingham RE, Haynes AC, Carr SA, Annan RS, McNulty DE, Liu WS, Terrett JA, Elshourbagy NA, Bergsma DJ, et al. (1998) Orexins and orexin receptors: a family of hypothalamic neuropeptides and G protein-coupled receptors that regulate feeding behavior. Cell 92:573–585.

Tanimura A, Yamazaki M, Hashimotodani Y, Uchigashima M, Kawata S, Abe M, Kita Y, Hashimoto K, Shimizu T, Watanabe M, Sakimura K, Kano M (2010) The endocannabinoid 2-arachidonoylglycerol produced by diacylglycerol lipase alpha mediates retrograde suppression of synaptic transmission. Neuron 65:320–327.

Tsou K, Brown S, Sañudo-Peña MC, Mackie K, Walker JM (1998) Immunohistochemical distribution of cannabinoid CB1 receptors in the rat central nervous system. Neuroscience 83:393–411.

Tsujino N, Sakurai T (2009) Orexin/hypocretin: a neuropeptide at the interface of sleep, energy homeostasis, and reward system. Pharmacol Rev 61:162–176.

Uchigashima M, Yamazaki M, Yamasaki M, Tanimura A, Sakimura K, Kano M, Watanabe M (2011) Molecular and morphological configuration for 2-arachidonoylglycerol-mediated retrograde signaling at mossy cell-granule cell synapses in the dentate gyrus. J Neurosci 31:7700–7714.

van den Pol AN (1999) Hypothalamic hypocretin (orexin): robust innervation of the spinal cord. J Neurosci 19:3171–3182.

van den Pol AN, Gao XB, Obrietan K, Kilduff TS, Belousov AB (1998) Presynaptic and postsynaptic actions and modulation of neuroendocrine neurons by a new hypothalamic peptide, hypocretin/orexin. J Neurosci 18:7962–7971.

Vaughan CW, Connor M, Bagley EE, Christie MJ (2000) Actions of cannabinoids on membrane properties and synaptic transmission in rat periaqueductal gray neurons in vitro. Mol Pharmacol 57:288–295.

Watanabe S, Kuwaki T, Yanagisawa M, Fukuda Y, Shimoyama M (2005) Persistent pain and stress activate pain-inhibitory orexin pathways. Neuroreport 16:5–8.

Wilson RI, Nicoll RA (2001) Endogenous cannabinoids mediate retrograde signalling at hippocampal synapses. Nature 410:588–592.

Xie X, Wisor JP, Hara J, Crowder TL, LeWinter R, Khroyan TV, Yamanaka A, Diano S, Horvath TL, Sakurai T, Toll L, Kilduff TS (2008) Hypocretin/orexin and nociceptin/orphanin FQ coordinately regulate analgesia in a mouse model of stress-induced analgesia. J Clin Invest 118:2471–2481.

Yoshida T, Uchigashima M, Yamasaki M, Katona I, Yamazaki M, Sakimura K, Kano M, Yoshioka M, Watanabe M (2011) Unique inhibitory synapse with particularly rich endocannabinoid signaling machinery on pyramidal neurons in basal amygdaloid nucleus. Proc Natl Acad Sci U S A 108:3059–3064.

Zucker RS, Regehr WG (2002) Short-term synaptic plasticity. Annu Rev Physiol 64:355–405.